AIMS Geosciences

AIMS Geosciences, 9(3): 595–608.
DOI: 10.3934/geosci.2023032
Received: 08 January 2023
Revised: 29 July 2023
Accepted: 29 August 2023
Published: 11 September 2023

http://www.aimspress.com/journal/geosciences

Research article

Rock strength degradation induced by salt precipitation: A new mechanical mechanism of sand production in ultra-deep fractured tight sandstone gas reservoirs

Dujie Zhang[1,2,3,*]

[1] State Key Laboratory of Shale Oil and Gas Enrichment Mechanisms and Effective Development, Beijing, P.R. China 100101
[2] Sinopec Research Institute of Petroleum Engineering, Beijing, P.R. China 10010
[3] Southwest Petroleum University, Chengdu, P.R. China 610500

* **Correspondence:** Email: zhangdj.sripe@sinopec.com.

Abstract: I take a typical ultra-deep tight sandstone gas reservoir located in Tarim Basin as an example to investigate the rare sand production problem. The situation of sand production was presented, and then conventional analyses were conducted. Six tight sandstone core plugs were selected to conduct rock mechanical tests before and after salt precipitation. Ultimately, a mathematical model was established to investigate the mechanism of rock strength degradation. The results of sand production prediction indicated that sand production from rock skeletons should never appear, but the rock skeletons was observed in the sand samples, and thus the impact of salt precipitation was taken into account. The experiments proved salt precipitation caused a degradation in rock strength, and the difference between actual- and predicted critical sand production pressure drop based on the weakened rock strength reduced significantly. Furthermore, the stress intensity factor on the fracture tip induced by salt precipitation reached up to 1.22 MPa·m$^{1/2}$, which was greater than the fracture toughness of tight sandstone, and it was used to explain the rock strength degradation. The results are helpful to the knowledge of the sand production problem in ultra-deep fractured tight sandstone gas reservoirs.

Keywords: ultra-deep; tight sandstone gas reservoirs; sand production; salt precipitation; rock strength degradation

1. Introduction

In the process of oil and gas reservoir exploitation, because of special geological conditions or complex construction processes, the structure of the reservoir rock around the wellbore changes dramatically, and the rock becomes more destructive. With the decrease of pore pressure, formation rock will break down and a lot of free sand grains will be produced. When the sand is carried into the wellbore or ground, it will cause a series of adverse effects on the normal production of oil and gas wells, and this phenomenon is called sand production [1,2]. In order to reduce the harm of sand production, proper sand control methods will be implemented during well completion and production. Because the mechanism of sand production is the basis of optimizing the sand control methods, a great deal of studies have been carried out on this problem.

In general, the fundamental mechanical mechanism of sand production can be summarized as two aspects: the failure or local plastic deformation of the rock induced by mechanical instabilities, and the shedding of rock particles from rock surface due to the fluid drag [3,4]. Nouri et al verified through hollow cylinder experiments that the detached materials from borehole well would be carried into the wellbore by the flow of fluid during sand production by the hollow cylinder sample experiments [5]. Younessi et al provided exhaustive experimental results to show that a minimum fluid flow rate was necessary for sand production rather than the yielding of the rock around borehole [6]. Numerous studies have shown that there are many factors influencing sand production, including rock mechanical properties, fluid flow velocity, fluid viscosity, variation of temperature and water saturation, drawdown pressure, perforation size, in-situ stress, multiphase flow and so on [7–13]. In general, sand production is a common problem in the weakly consolidated sandstone reservoirs. Due to a high degree of rock consolidation and high rock mechanical strength, it was generally assumed that sand production was not an issue for tight sandstone reservoirs. As far as I know, little research has been done on sand production in tight sandstone.

However, with the development of deep and ultra-deep tight sandstone gas reservoirs, sand production has become a severe problem in this type reservoir [14,15]. Take the ultra-deep tight sandstone gas reservoirs located on the north side of Tarim Basin as an example. The buried depth of the main pay zone is 6500 ~ 8000 m, and the maximum effective thickness is 150 m. The reservoir sandstones are lithic arkose sandstone and feldspar lithic sandstone. The permeability is approximately 0.001 ~ 0.5 mD, and the porosity is 2 ~ 7 %. As shown in Figure 1, the cumulative number of sand wells in the gas field has risen to 26, which poses a severe challenge for the stable productivity of the gas reservoir. Understanding the mechanism of sand production so as to provide a theoretical basis for sand production control is increasingly urgent.

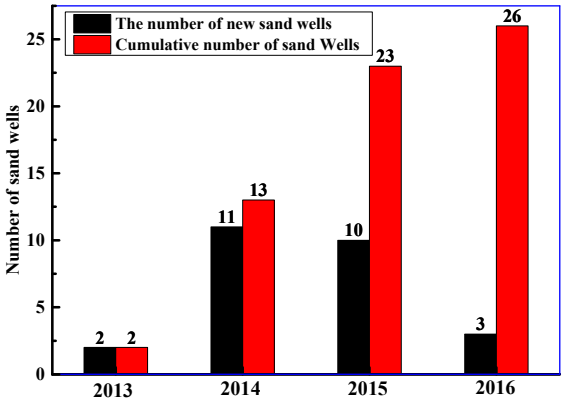

Figure 1. The number of the sand production wells in the ultra-deep tight sandstone gas reservoirs in Tarim Baisn.

I take the K gas field, a typical ultra-deep tight sandstone gas reservoir located in Tarim Basin, China, as an example. In this paper, the composition of the output sand from the gas field was analyzed first. Then, the conventional sand production prediction method was used to identify the probability of sand production. Subsequently, a series of rock mechanical tests of tight sandstone before and after salt precipitation were conducted and used for sand production analysis for the first time. Based on the experimental results, the criterion for sand production was recalculated. The result was helpful for further research on the sand production mechanism and sand prevention in the ultra-deep fractured tight sandstone gas reservoirs.

2. Conventional analysis of sand production

2.1. Qualitative prediction of sand production

There are many methods to make predictions on sand production. Among them, the empirical method was considered to be simple and quick, including the Combined modulus method, Schlumberger method, Porosity index method and Sonic differential time method. Thus, I needed to have a preliminary understanding of the problem of sand production in K gas field. The gas reservoir is located in Kelasu structure belt, which is located on the north side of Keshen depression, north part of Tarim Basin. The reservoir was under the double effects of diagenetic compaction and tectonic compression. The main sedimentary facies types are braid river deposits. Its lithology is sandstone of braid delta facies and effective thickness is up to 150 m. Lithic content ranges from 18~22%, and 19.4% on average. The filling in the sandstone reservoir include silica and calcareous. As an overpressure reservoir, the pressure coefficient ranges from 1.75 to 1.80. The geothermal gradient of the reservoirs is normal, which is 2.20 ~ 2.30 ℃/100m. A typical sand production well was selected. Based on the well log data, the above four empirical methods were used to determine whether the well would produce sand, and the results are shown in Figure 2. The results indicated that the Porosity index ranged from 4 ~ 10%, which was well below the critical sand-producing porosity (20%); the Sonic differential time ranged from 180 ~ 210 μs/m, which was below the critical value (321 μs/m); the Combined modulus ranged from

$55 \times 10^3 \sim 80 \times 10^3$ MPa, which was well above the critical value (20×10^3 MPa); the Schlumberger rate ranged from 62 ~ 120 GPa^2, which was well above the critical value (62 GPa^2). It is not difficult to see that sand production from rock skeletons was not going to happen. It is evident that sand production from rock skeletons was not going to happen. Therefore, the composition of the output sand obtained from the wellhead was analyzed.

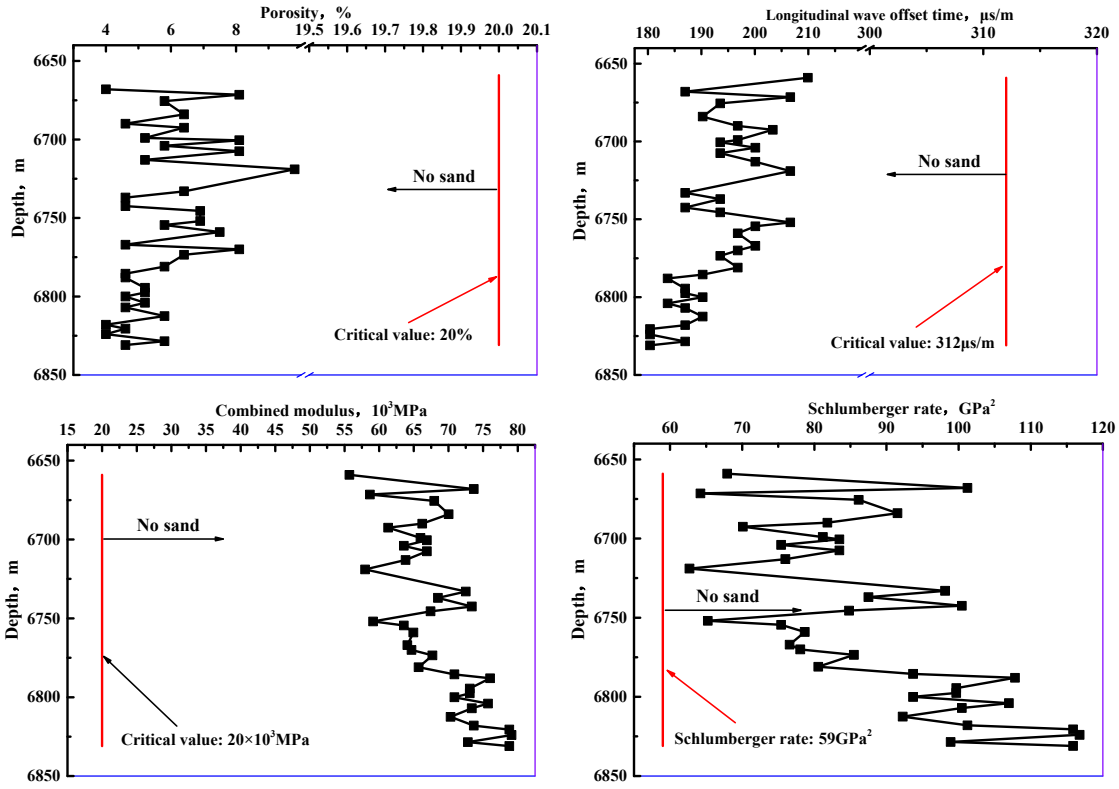

Figure 2. Empirical prediction results for sand production of ultra-deep tight sandstone gas reservoirs in Tarim Baisn.

2.2. Composition of the output sand

The sand samples obtained from the wellhead are shown in Figure 3. From the appearance of the output sand, the particle size distribution of the output sand was very wide, not only nano-micron particles, but also a few centimeters in diameter. In terms of composition, the output sand mainly included cement blocks, cement chips, fracturing sand, iron chips and formation skeleton sand.

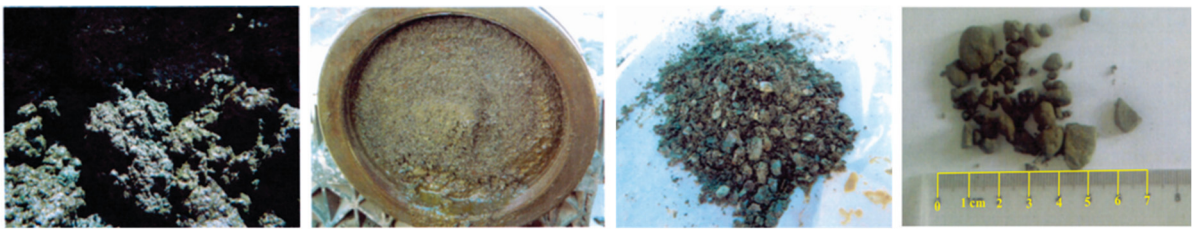

Figure 3. The samples of produced sand particles from the K gas field.

Preliminary analysis indicated that the concrete blocks and iron chips in the output sand can be described to the failure of the cement ring and casing in the production process due to the poor cementing quality. The fracturing sand can be attributed to the backflow of the fracturing proppant and the crushing proppant particles caused by the closure of the fracture induced by the high ground stress. It is strange that where the formation skeleton sand come from, which is not consistent with the qualitative prediction results of sand production.

Usually, the production pressure drop is considered to have a great impact on sand production. In order to further investigate this problem, I calculated the critical production pressure drop by M-C strength criterion method, D-P strength criterion method and C-Index method, respectively. Because of the reservoir rock strength, in-situ stress gradient and pore-pressure gradient are close, thus I considered only the changes in buried depth and unified other parameters in the calculation model, and the parameters used by the model were: $\sigma_v / H_w = 2.45$; $\sigma_H / H_w = 2.77$; $\sigma_h / H_w = 2.14$; $p_0 / H_w = 1.62$; $\mu = 0.229$; $\beta = 0.38$; $S_0 = 9.76MPa$; $\varphi = 19.25^\circ$; $\sigma_c = 115.30MPa$, where σ_v is the vertical wellbore stress, MPa; σ_H is the maximum horizontal principal stress, MPa; σ_h is the minimum horizontal principal stress, MPa; p_0 is pore pressure, MPa; μ is Poisson's ratio; β is Biot coefficient; S_0 is rock joint cohesion, MPa; φ is internal friction angle, rad; σ_c is the uniaxial compressive strength，MPa; H_w is the depth of the formation, m. The calculation results are shown in Table 1. According to the prediction of C-Index method, D-P strength criterion method and M-C strength criterion method, the difference between the actual sand production pressure drop and the predicted the critical sand production pressure drop ranged from 22.87 ~ 38.74 MPa, 24.57 ~ 42.07 MPa and 55.98 ~ 74.05 MPa, respectively. The calculation results show that it was almost impossible for sand production to occur in this formation, which was not consistent with the field practice.

Table 1. Comparison of the actual sand production pressure drop and the predicted critical sand production pressure drop.

Well no.	Depth, m	Degree of sand production	Predicted critical sand production pressure drop, MPa			Actual sand production pressure drop, MPa
			M-C method	D-P method	C-Index	
KS2-2-14	6523~6975	Severity	74.91~79.17	43.79~47.19	42.90~43.86	＜5.12
KS2-2-12	6600~6807		76.20~77.58	44.80~45.91	43.26~43.57	＜5.43
KS2-1-1	6670~6825		76.29~77.75	44.88~46.05	43.22~43.55	＜11.30
KS2-2-5	6663~6927		76.23~78.71	44.83~46.82	43.01~43.56	＜6.49
KS2-2-20	6733~6887		76.89~78.34	45.35~46.52	43.09~43.42	＜19.30
KS2-2-18	6669~6850		76.28~77.99	44.87~46.24	43.17~43.55	＜20.30
KS2-1-14	6776~7016		77.29~79.55	45.68~47.50	42.82~43.33	＜8.60
KS2-1-8	6567~6767	Medium	75.32~77.21	44.11~45.61	43.34~43.77	＜3.10
KS2-2-8	6583~6853	Minor	75.47~78.02	44.23~46.36	43.16~43.73	15.30

2.3. Salt precipitation in the gas reservoir

Preliminary analysis suggested that the theoretical basis of the qualitative prediction method of sand production is the mechanical properties of the rock, and the rock mechanics parameters used in the model were obtained from the original formation. However, the rock mechanics parameters were

always changing during gas production. In general, the intrusion of external fluid into the formation could easily lead to the reduction of rock mechanical strength. However, in the process of gas reservoir production, the rock strength reduction induced by similar reasons could not be considered because there is almost no working fluid entry after the drilling is over. However, it should be noted that due to the large depth of the formation, the formation water salinity analysis shows that the water salinity of the gas reservoir is higher, more than 21000 mg/L. In the process of gas reservoir production, some water vapor was taken away due to the continuous production of natural gas, resulting in the precipitation of a large number of inorganic salts dissolved in formation water, and finally deposited in the gas reservoir. This was also known as salt precipitation. As stated in previous literature [16], salt precipitation is a common phenomenon encountered in many engineering endeavors, including the control of water loss from land surfaces, protection of pavements, roads and historical monuments [17] and various geochemical issues related to intact geological formations [18]. The mechanism for salt precipitation in deep geological formations is more complex than those encountered on surficial soils. For example, CO_2 sequestration enhanced geothermal systems and natural gas production are all situations. In the oil and gas reservoirs with high salinity formation water, salt precipitation around the wellbore was always serious [19,20]. According to the experimental results, Noiriel et al found that sodium chloride precipitation in tight sandstone induced rock failure [21]. From this, I can infer that the rock strength would decrease induced by salt precipitation during gas production. More daringly, could it be that the rock strength degradation induced by salt precipitation leads to sand production? To test this hypothesis, a series of rock mechanical tests of the tight sandstone before and salt precipitation were carried out.

3. Experimental studies

3.1. Sample preparation

The tight sandstone cores were taken from Bashijiqi formation of Cretaceous in K gas field, which was made into cylindrical plugs of 45 ~ 50 mm in height and 25 mm in diameter. Before experiments, the core plugs were placed in an oven of 60 ℃ until the weight of the samples did not change. Then, porosity, permeability and acoustic velocity of the core plugs were measured. Ultimately, the core plugs with similar parameters were selected for subsequent experiments. The physical properties of the core plugs are shown in Table 2.

Table 2. The basic physical properties of the tight sandstone core plugs.

Core no.	Depth (m)	L (mm)	D (mm)	ϕ (%)	K (mD)
UD6-7	7764.99	50.98	25.26	2.48	0.01910
UD7-14	7738.86	50.32	25.26	3.70	0.01311
UD1-10	7734.67	49.28	25.26	3.38	0.00588
UD6-1	7647.19	50.22	25.26	3.09	0.02660
UD8-13	7770.78	49.98	25.26	2.69	0.02250
UD8-20	7768.04	49.43	25.26	2.41	0.01217

The simulated formation water used in the experiments was made in the lab on the basis of the analysis of the elementary composition of the formation water obtained from gas reservoirs, as shown in Table 3.

Table 3. Elemental analysis of the formation water.

Inorganic salt types	$NaHCO_3$	Na_2SO_4	NaCl
Content (mg/L)	243.6	604.9	171497.0
Inorganic salt types	$MgCl_2$	$CaCl_2$	Total salinity
Content (mg/L)	3744.0	28837.8	204927.3

3.2. Experimental facility

RTR-1000 Electro-hydraulic Servo Triaxial Rock Mechanics Testing System (GCTS Co., USA) was used to carry out the rock mechanical tests. The maximum axial pressure was 1000 KN, the maximum confining pressure was 140 MPa and the dynamic frequency was 10 Hz. FEI Quanta 450 SEM (FEI Co., USA) was used to characterize the distribution of crystalline salt after rock mechanical test, and the resolution is 3 nm at 30 kV.

3.3. Experimental procedures

Detailed experimental procedures are described below: ① Selected tight sandstone core plugs and then measured the length, diameter, porosity, permeability and acoustic velocity. ② Selected the tight sandstone core plugs with similar physical properties and then divided them into two groups (3 + 3), representing the condition of before and after salt precipitation, respectively. ③ Saturated one group of core plugs with formation water completely. ④ Carried out uniaxial compression tests (1 + 1) and triaxial compression tests (2 + 2). ⑤ Carried out the experiment of Scanning Electron Microscopy on the cores after salt precipitation. In addition, through the analysis of the mineral composition of the rocks, it was found that the rocks are mainly quartz, feldspar and cuttings. According to previous studies, the change of experimental temperature has a little effect on the rock strength of this kind of quartz sandstone, especially when the temperature is lower than 200 ℃. In addition, mechanical degradation of rock caused by the physiochemically such as osmosis was mainly caused by hydration of clay minerals in rocks. However, the clay mineral content of the rock samples is very low. Therefore, the influence of physical parameters, such as cyclic flushing and temperature change, or physiochemically, such as osmosis, on the mechanical degradation can be excluded.

4. Results

4.1. Experimental results of rock mechanics

The results of the uniaxial compression tests on the tight sandstone before and after salt precipitation are shown in Figure 4. As shown in the figure, the uniaxial stress-strain curve of tight sandstone moved down. The slope of the elastic segment decreases significantly, and the peak differential stress decreased significantly as well. The results of the quantitative analyses indicated that

Young's elastic modulus of tight sandstone decreased from 16.787 GPa to 10.217 GPa, and the Poisson's ratio increased up from 0.100 to 0.129. In addition, the rock compressive strength reduced from 115.3 MPa to 75.90 MPa.

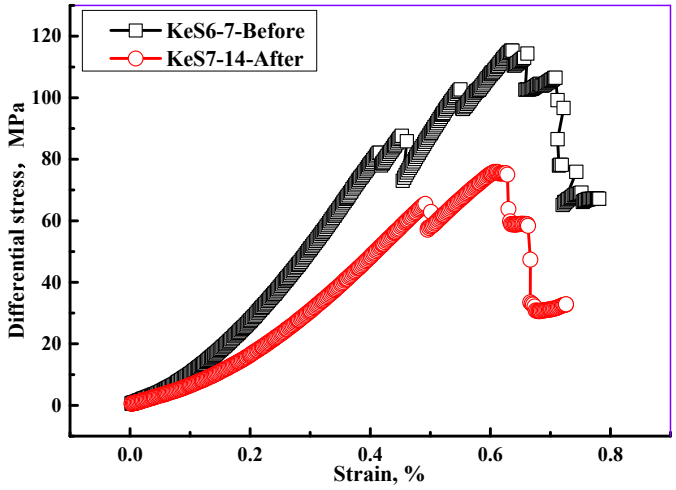

Figure 4. The uniaxial stress strain curve of the samples before and after salt precipitation.

The results of triaxial compression tests on the tight sandstone core plugs before and after salt precipitation are shown in Figure 5. As shown in the figure, the triaxial stress-strain curves of tight sandstone also moved down. The slopes of the elastic segment decreased significantly, and the peak differential stress decreased significantly as well. The results indicated that Young's elastic modulus, cohesion and internal friction angle all decreased after salt precipitation, and the Poisson's ratio increased. It is not hard to see that salt precipitation did cause a degradation in the strength of the formation rock.

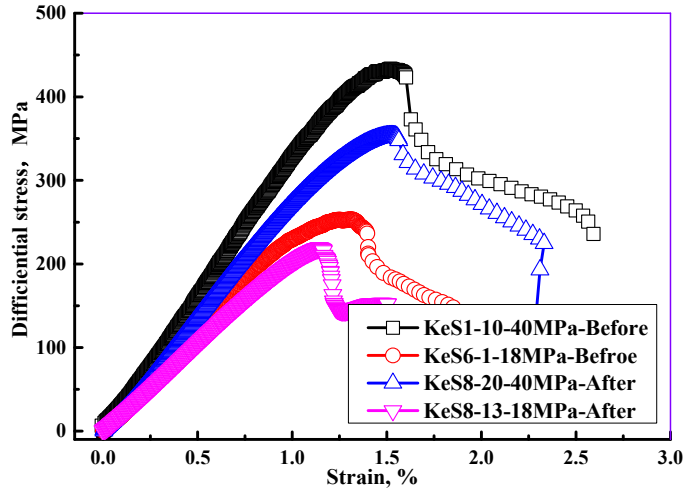

Figure 5. The triaxial stress strain curve of the samples before and after salt precipitation.

4.2. Characterization of crystalline salt

In order to further study the mechanism of rock strength degradation induced by salt precipitation, the morphology and distribution of crystalline salt in the tight sandstone cores were observed by SEM, and the typical SEM image is shown in Figure 6. As shown in this figure, large amounts of crystalline salt appeared on the rock surface, and most of the crystalline salt filled the microfractures. In general, fracture is thought to be more prone to failure with the increase of pore pressure. Thus, I speculated that it may be the failure of fracture induced by salt precipitation that leads to the rock strength degradation. However, whether the crystallization stress induced by crystallization salt in the fracture could cause the failure of the fracture requires a theoretical derivation.

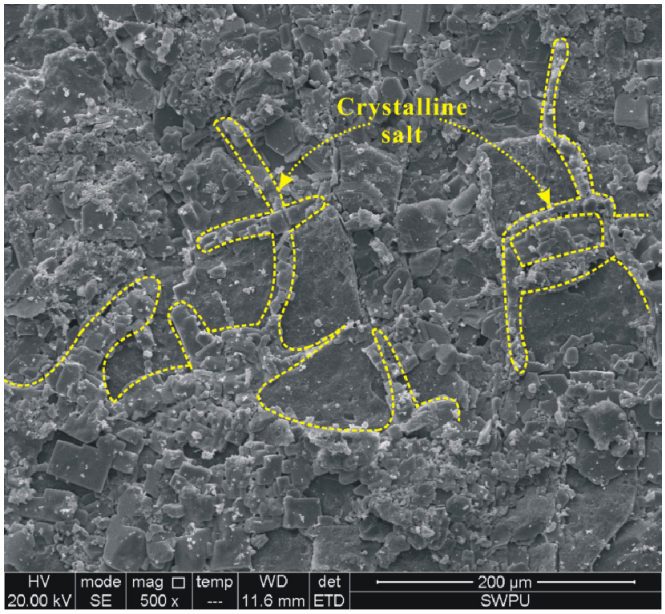

Figure 6. Scanning electron microscope image of the crystalline salt after salt precipitation.

5. Discussion

5.1. Sand production prediction considering rock strength degradation

According to the results of Uniaxial/Triaxial compression tests, the critical production pressure drop was also calculated based on M-C strength criterion method, D-P strength criterion method and C-Index method, respectively. Because of the reservoir rock strength, in-situ stress gradient and pore-pressure gradient are close. Therefore, I considered only the changes in buried depth and unified other parameters in the calculation model for the sand producing wells in K gas reservoir. The parameters used by the model were $\sigma_v / H_w = 2.45$; $\sigma_H / H_w = 2.77$; $\sigma_h / H_w = 2.14$; $p_0 / H_w = 1.62$; $\mu = 0.229$; $\beta = 0.38$; $S_0 = 9.76MPa$; $\phi = 19.25^\circ$; $\sigma_c = 75.90MPa$, and the calculation results are shown in Table 4. According to the results of C-Index method, D-P strength criterion method and M-C strength criterion method, the difference between the actual sand production pressure drop and the predicted critical sand production pressure drop considering rock strength degradation ranged from 0.76 ~ 16.75 MPa, 5.22 ~ 21.88 MPa and 45.71 ~ 63.38 MPa, respectively, which showed that the difference reduced

significantly. Thus, the rock strength degradation induced by salt precipitation did cause sand production to some extent in this gas field. However, due to the complexity of the problem, the indefinite of the factors and the limits of the predicting method, the difference between the actual sand production pressure drop and the predicted critical sand production pressure drop still existed and required further study.

Table 4. Comparison of the actual sand production pressure drop and the predicted critical sand production pressure drop considering rock strength degradation.

Well no.	Depth, m	Degree of sand production	Predicted critical sand production pressure drop, MPa			Actual sand production pressure drop, MPa
			M-C method	D-P method	C-Index	
KS2-2-14	6523~6975	Severity	64.83~68.50	24.82~27.00	20.75~21.87	＜5.12
KS2-2-12	6600~6807		65.94~67.14	25.47~26.18	21.17~21.53	＜5.43
KS2-1-1	6670~6825		66.02~67.28	25.52~26.27	21.12~21.51	＜11.30
KS2-2-5	6663~6927		65.97~68.11	25.49~26.77	20.87~21.52	＜6.49
KS2-2-20	6733~6887		66.54~67.79	25.82~26.57	20.97~21.35	＜19.30
KS2-2-18	6669~6850		66.01~67.49	25.52~26.39	21.06~21.51	＜20.30
KS2-1-14	6776~7016		66.89~68.94	26.03~27.21	20.65~21.25	＜8.60
KS2-1-8	6567~6767	Medium	65.18~66.81	25.03~25.99	21.27~21.76	＜3.10
KS2-2-8	6583~6853	Minor	65.31~67.51	25.11~26.41	21.06~21.72	15.30

5.2. The mechanism of rock strength degradation induced by salt precipitation

In order to determine whether the crystallization stress induced by crystallization salt in the fracture could cause the failure of fracture, a simplified mechanical model was established based on the distribution of the crystalline salt, and the model is shown in Figure 7. Theory of fracture mechanics was used to predicting the critical failure condition, and the criterion for failure is:

$$K_I = K_{IC} \tag{1}$$

where K_I is stress intensity factor, and K_{IC} is the fracture toughness of tight sandstone.

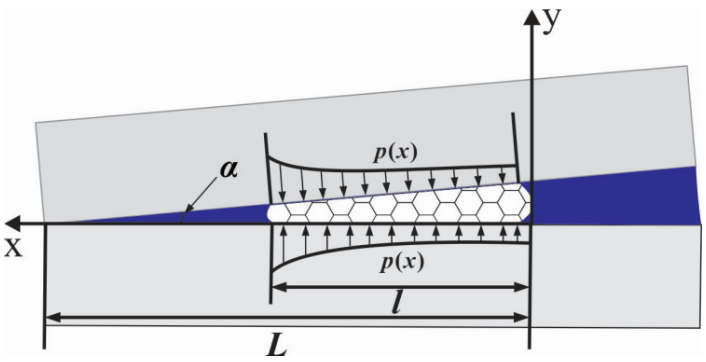

Figure 7. The distribution of crystallization stress in the wedge fracture [13].

According to coordinate conversion, the distribution function of the crystallization stress on the fracture surface is:

$$p = \frac{\gamma_{CL}}{(L-l)\tan(\alpha/2)} \tag{2}$$

where p is crystallization stress, γ_{CL} is interfacial free energy of sodium chloride, L is the distance between the tip of fracture and the location of salt precipitation, l is the length of the crystalline salt and α is fracture opening angle. The stress intensity factor on the fracture tip is described by the following equation:

$$K_{\mathrm{I}} = \frac{1}{\sqrt{\pi L}} \int_0^L p(l) \left(\frac{L+l}{L-l} \right)^{1/2} dl \tag{3}$$

Substituting Eq. (2) into Eq. (3), I got the formula of the stress intensity factor on the fracture tip considering crystallization stress:

$$K_{\mathrm{I}} = \frac{\gamma_{CL}}{\tan(\alpha/2)\sqrt{\pi L}} \int_0^L \frac{1}{L-l} \left(\frac{L+l}{L-l} \right)^{1/2} dl \tag{4}$$

According to the actual situation of K gas field, I assumed that the crystalline salt was sodium chloride, $L = 1.5$ m, $\gamma_{CL} = 0.1\ J/m^2$, and the fracture-opening angle was set to 0.1°, 0.2°, 0.3°, 0.4° and 0.5°, respectively. The calculation results are shown in Figure 8.

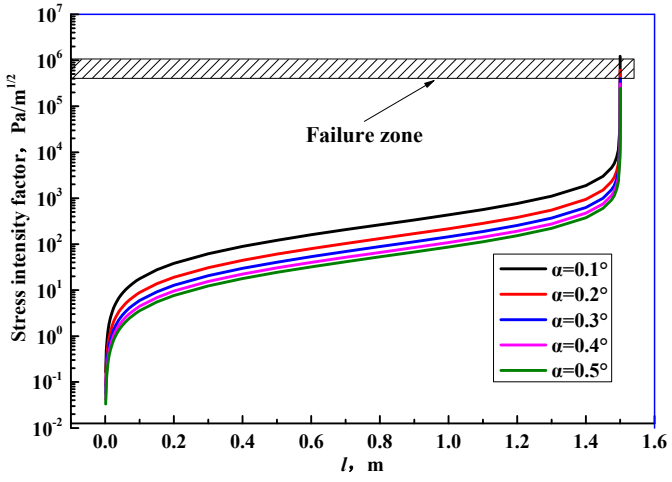

Figure 8. Stress intensity factor changes induced by crystallization salt at different locations in wedge fractures.

As shown in this figure, when the fracture opening angle was 0.1°, $L-l = 5$ μm, the stress intensity factor can reach up to 1.22 MPa·m$^{1/2}$, which was greater than the fracture toughness of tight sandstone (0.3 ~ 1.0 MPa·m$^{1/2}$) [22]. From this, it can be known that the crystallization stress induced by the

crystallization of sodium chloride in the fracture will cause the failure of fracture, and then lead to the strength degradation of tight sandstone.

6. Conclusions

I take an ultra-deep tight sandstone gas reservoir in Tarim Basin, China as an example to investigate the problem of sand production. The results of the qualitative predictions of sand production indicated that sand production from rock skeletons was not an issue in the gas reservoir, but the rock skeleton sand was observed from the produced sand samples. The critical sand production pressure drops obtained by M-C strength criterion method, D-P strength criterion method and C-Index method were greater than the actual sand production pressure drop in the gas field, and then salt precipitation was considered to have a serious impact. The results of uniaxial/triaxial compression tests indicated that the salt precipitation caused a degradation in the strength of the tight sandstone. Then, based on the weakened rock strength, the critical sand production pressure drop was calculated again, and the difference between actual sand production pressure drop and the predicted sand critical sand production pressure drop reduced significantly. SEM image showed that the crystalline salt filled the microfractures, and then a simplified mechanical model was established to investigate the possibility of the failure of a fracture induced by salt precipitation. The results indicated that the stress intensity factor on the fracture tip can reach up to 1.22 $MPa \cdot m^{1/2}$ induced by salt precipitation, which was greater than the fracture toughness of tight sandstone.

Use of AI tools declaration

The authors declare they have not used Artificial Intelligence (AI) tools in the creation of this article.

Acknowledgements

This paper is supported by National Natural Science Foundation of China "Basic theory and method of high temperature and high-pressure oil and gas safe and efficient drilling and completion engineering (Grant No. U19B6003-05)" and National Key Research and Development Plan Project "Closed-loop response Mechanism and intelligent control Method of Wellbore Stability (Grant No. 2019YFA0708303)".

Conflict of interest

All authors declare no conflicts of interest in this paper.

References

1. Rahmati H, Mahshid J, Saman A, et al. (2013) Review of sand production prediction models. *J Pet Eng* 2013: 864981. https://doi.org/10.1155/2013/864981

2. Cui Y, Nouri A, Chan D, et al. (2016) A new approach to DEM simulation of sand production. *J Pet Sci Eng* 147: 56–67. https://doi.org/10.1016/j.petrol.2016.05.007
3. Vardoulakis I, Stavropoulou M, Papanastasiou P (1996) Hydro-mechanical aspects of the sand production problem. *Transp Porous Media* 22: 225–244. https://doi.org/10.1007/BF01143517
4. Li X, Feng Y, Gray KE (2018) A hydro-mechanical sand erosion model for sand production simulation. *J Pet Sci Eng* 166: 208–224. https://doi.org/10.1016/j.petrol. 2018.03.042
5. Nouri A, Vaziri H, Belhaj H, et al. (2006) Sand-production prediction: a new set of criteria for modeling based on large-scale transient experiments and numerical investigation. *SPE J* 11: 227–237. https://doi.org/10.2118/90273-PA
6. Younessi A, Rasouli V, Wu B (2013) Sand production simulation under true-triaxial stress conditions. *Int J Rock Mech Min Sci* 61: 130–140. https://doi.org/10.1016/j.ijrmms.2013.03.001
7. Boutt DF, Cook BK, Williams JR (2011) A coupled fluid–solid model for problems in geomechanics: application to sand production. *Int J Numer Anal Methods Geomech* 35: 997–1018. https://doi.org/10.1002/nag.938
8. Fattahpour V, Moosavi M, Mehranpour M (2012) An experimental investigation on the effect of rock strength and perforation size on sand production. *J Pet Sci Eng* 86: 172–189. https://doi.org/10.1016/j.petrol.2012.03.023
9. Ranjith PG, Perera MSA, Perera WKG, et al. (2013) Effective parameters for sand production in unconsolidated formations: An experimental study. *J Pet Sci Eng* 105: 34–42. https://doi.org/10.1016/j.petrol.2013.03.023
10. Gravanis E, Sarris E, Papanastasiou P (2015) Hydro-mechanical erosion models for sand production. *Int J Numer Anal Methods Geomech* 39: 2017–2036. https://doi.org/10.1002/nag.2383
11. Wang H, Gala DP, Sharma MM (2018) Effect of fluid type and multiphase flow on sand production in oil and gas wells. *SPE J* 24: 733–743. https://doi.org/10.2118/187117-PA
12. Ranjith PG, Perera MSA, Perera WKG, et al. (2013) Effective parameters for sand production in unconsolidated formations: An experimental study. *J Pet Sci Eng* 105: 34–42. https://doi.org/10.1016/j.petrol.2013.03.023
13. Abdelghany WK, Hammed MS, Radwan AE (2023) Implications of machine learning on geomechanical characterization and sand management: a case study from Hilal field, Gulf of Suez, Egypt. *J Pet Explor Prod Technol* 13: 297–312. https://doi.org/10.1007/s13202-022-01551-9
14. Yang X, Jin X, Zhang Y, et al. (2016) Investigating the fundamental mechanisms governing solid production in super-deep hot tight gas reservoirs and exploring potential solutions. In *SPE Annual Technical Conference and Exhibition*, Dubai, UAE (SPE-181731-MS). https://doi.org/10.2118/181731-MS
15. Ou Q, Yang J, Zhang Z, et al. (2021) Prediction of high-temperature and high-pressure well sand production in the DF gas field. In *ARMA US Rock Mechanics/Geomechanics Symposium* (ARMA-2021). ARMA. https://doi.org/10.2118/191406-PA
16. Zhang D, Kang Y, Selvadurai APS, et al. (2020) Experimental investigation of the effect of salt precipitation on the physical and mechanical properties of a tight sandstone. *Rock Mech Rock Eng* 53: 4367–4380. https://doi.org/10.1007/s00603-019-02032-y

17. Espinosa-Marzal RM, Scherer GW (2013) Impact of in-pore salt crystallization on transport properties. *Environ Earth Sci* 69: 2657–2669. https://doi.org/10.1007/s12665-012-2087-z
18. Shahidzadeh-Bonn N, Desarnaud J, Bertrand F, et al. (2010) Damage in porous media due to salt crystallization. *Phys Rev E* 81: 066110. https://doi.org/10.1103/PhysRevE.81.066110
19. Kleinitz W, Koehler M, Dietzsch G (2001) The precipitation of salt in gas producing wells. In SPE European formation damage conference (SPE-68953-MS). SPE. https://doi.org/10.2118/68953-MS
20. Eppelbaum LV, Yakubov YS, Ezersky M (2010). Method for comprehensive computing of water flows geodynamics in the Dead Sea basin. In *Near Surface 2010-16th EAGE European Meeting of Environmental and Engineering Geophysics* (164). https://doi.org/10.3997/2214-4609.20144866
21. Noiriel C, Renard F, Doan ML, et al. (2010) Intense fracturing and fracture sealing induced by mineral growth in porous rocks. *Chem Geol* 269: 197–209. https://doi.org/10.1016/j.chemgeo.2009.09.018
22. Coussy O (2010) Mechanics and Physics of Porous Solids. John Wiley, Chichester, U. K. https://doi:10.1002/9780470710388

AIMS Press